

Lepton Asymmetries in Heavy Baryon Decays of $\Lambda_b \rightarrow \Lambda l^+ l^-$

Chuan-Hung Chen^a and C. Q. Geng^b

^a*Department of Physics, National Cheng Kung University
Tainan, Taiwan, Republic of China*

^b*Department of Physics, National Tsing Hua University
Hsinchu, Taiwan, Republic of China*

Abstract

We study the dilepton forward-backward and the longitudinal, normal and transverse lepton polarization asymmetries in the heavy baryon decays of $\Lambda_b \rightarrow \Lambda l^+ l^-$. We show that the asymmetries have a less dependence on the non-perturbative QCD effects. In the standard model, we find that the integrated forward-backward asymmetries (FBAs) and three components of the polarizations in the QCD sum rule approach (pole model) are -0.13 (-0.12) and $(58.3, -9.4, -0.07)\%$ ($(58.3, -12.6, -0.07)\%$) for $\Lambda_b \rightarrow \Lambda \mu^+ \mu^-$ and -0.04 (-0.03) and $(10.9, -10.0, -0.39)\%$ ($(10.9, -0.2, -0.34)\%$) for $\Lambda_b \rightarrow \Lambda \tau^+ \tau^-$, respectively.

1 Introduction

It is known that the FBAs of the dileptons in the inclusive decays of $b \rightarrow sl^+l^-$ provide us with information on the short-distance (SD) contributions, which are dominated by the top quark loops in the standard model [1]. The longitudinal lepton polarizations in $b \rightarrow sl^+l^-$, which are another parity violating observables, are also interesting asymmetries. In particular, the tau polarization in $b \rightarrow s\tau^-\tau^-$ could be accessible to the B-Factories [2, 3]. It is noted that the FBAs of the exclusive decays $B \rightarrow Ml^+l^-$ are identically zero when M are pseudoscalar mesons such as π and K but nonzero for M being vector mesons such as ρ and K^* . However, the longitudinal lepton polarizations [4] as well as other components [5] are nonzero for both types of the exclusive B meson decay modes.

In this paper, we study the dilepton forward-backward and various lepton polarization asymmetries in the heavy baryon decays of $\Lambda_b \rightarrow \Lambda l^+l^-$. To study these baryonic decays, one of the most difficulties is to evaluate the hadronic matrix elements. It is known that there are many form factors for the $\Lambda_b \rightarrow \Lambda$ transition, which are hard to be calculated since they are related to the non-perturbative effect of QCD. However, in heavy particle decays, the heavy quark effective theory (HQET) could reduce the number of form factors and supply the information with respect to their relative size [6, 7, 8]. With the HQET, we shall use the QCD sum rule approach [6] and the pole model [9] in our numerical calculations for the form factors.

The paper is organized as follows. In Sec. 2, we study the effective Hamiltonian for the decays of $\Lambda_b \rightarrow \Lambda l^+l^-$ ($l = e, \mu, \tau$) and form factors in the $\Lambda_b \rightarrow \Lambda$ transition. In Sec. 3, we derive the general forms of the lepton polarization and dilepton forward-backward asymmetries in $\Lambda_b \rightarrow \Lambda l^+l^-$. We give our numerical analysis in Sec. 4. In Sec. 5, we present our conclusions.

2 Effective Hamiltonian and Form factors

To study the heavy baryon decays of $\Lambda_b \rightarrow \Lambda l^+l^-$ ($l = e$ or μ or τ), we start with the effective Hamiltonian for the b -quark decay of $b \rightarrow sl^+l^-$, given by

$$\mathcal{H} = -4 \frac{G_F}{\sqrt{2}} V_{tb} V_{ts}^* \sum_{i=1}^{10} C_i(\mu) O_i(\mu) \quad (1)$$

where G_F is the Fermi constant, V_{ij} are the CKM matrix elements, and $C_i(\mu)$ and $O_i(\mu)$ are the expressions for the renormalized Wilson coefficients and operators, whose expressions can be found in Ref. [10], respectively. In terms of the Hamiltonian in Eq. (1), the free quark decay amplitude is written as

$$\begin{aligned} \mathcal{M}(b \rightarrow sl^+l^-) = & \frac{G_F \alpha_{em}}{\sqrt{2\pi}} V_{tb} V_{ts}^* \left[\bar{s} \left(C_9^{eff}(\mu) \gamma_\mu P_L - \frac{2m_b}{q^2} C_7(\mu) i\sigma_{\mu\nu} q^\nu P_R \right) b \bar{l} \gamma^\mu l \right. \\ & \left. + \bar{s} C_{10} \gamma_\mu P_L b \bar{l} \gamma^\mu \gamma_5 l \right] \end{aligned} \quad (2)$$

with $P_{L(R)} = (1 \mp \gamma_5)/2$. We note that in Eq. (2), only the term associated with the Wilson coefficient C_{10} is independent of the μ scale. We also note that the dominant contribution to the decay rate is from the long-distance (LD), such as that from the $c\bar{c}$ resonant states of Ψ, Ψ', \dots etc. It is known that to find out the LD effects for the B-meson decays, in the

literature [1, 3, 4, 11, 12, 13], both the factorization assumption (FA) and the vector meson dominance (VMD) approximation have been used. For the LD contributions in baryonic decays, we assume that the parametrization is the same as that in the B meson decays. Hence, we may include the resonant effect (RE) by absorbing it to the corresponding Wilson coefficients. The effective Wilson coefficient of C_9^{eff} has the standard form

$$C_9^{eff} = C_9(\mu) + (3C_1(\mu) + C_2(\mu)) \left(h(x, s) + \frac{3}{\alpha_{em}^2} \sum_{j=\Psi, \Psi'} k_j \frac{\pi \Gamma(j \rightarrow l^+ l^-) M_j}{q^2 - M_j^2 + i M_j \Gamma_j} \right)$$

where $h(x, s)$ describes the one-loop matrix elements of operators $O_1 = \bar{s}_\alpha \gamma^\mu P_L b_\beta \bar{c}_\beta \gamma_\mu P_L c_\alpha$ and $O_2 = \bar{s} \gamma^\mu P_L b \bar{c} \gamma_\mu P_L c$ as shown in Ref. [10], M_j (Γ_j) are the masses (widths) of intermediate states, and the factors k_j are phenomenological parameters for compensating the approximations of FA and VMD and reproducing the correct branching ratios of $B(B \rightarrow J/\Psi X \rightarrow l^+ l^- X) = B(B \rightarrow J/\Psi X) \times B(J/\Psi \rightarrow l^+ l^-)$. In this paper we take the Wilson coefficients at the scale of $\mu \sim m_b \sim 5.0$ GeV and their values are taking to be $C_1(m_b) = -0.226$, $C_2(m_b) = 1.096$, $C_7(m_b) = -0.305$, $C_9(m_b) = 4.186$, and $C_{10}(m_b) = -4.599$, respectively.

It is clear that one of the main theoretical uncertainties in studying exclusive decays arises from the calculation of form factors. With the HQET, the hadronic matrix elements for the heavy baryon decays could be parametrized as follows [9]

$$\langle \Lambda(p, s) | \bar{s} \Gamma b | \Lambda_b(v, s') \rangle = \bar{u}_\Lambda(p, s) \left\{ F_1(q^2) + \not{v} F_2(q^2) \right\} \Gamma u_{\Lambda_b}(v, s') \quad (3)$$

where $v = p_{\Lambda_b}/M_{\Lambda_b}$ is the four-velocity of the heavy baryon, $q^2 = (p_{\Lambda_b} - p_\Lambda)^2$ is the square of the momentum transform, and Γ denotes the possible Dirac matrix. Note that in terms of the HQET there are only two independent form factors, F_1 and F_2 , in Eq. (3) for each Γ . In the following, we shall use F_1 and $R \equiv F_2/F_1$ as the two independent parameters and adopt the HQET approximation to analyze the behavior of $\Lambda_b \rightarrow \Lambda l^+ l^-$.

From Eqs. (2) and (3), the transition matrix element for $\Lambda_b(p_{\Lambda_b}) \rightarrow \Lambda(p_\Lambda) l^+(p_+) l^-(p_-)$ can be expressed as

$$\mathcal{M}(\Lambda_b \rightarrow \Lambda l^+ l^-) = \frac{G_F \alpha_{em}}{\sqrt{2\pi}} V_{tb} V_{ts}^* [H_{1\mu} L_V^\mu + H_{2\mu} L_A^\mu] \quad (4)$$

with

$$\begin{aligned} L_V &= \bar{l} \gamma^\mu l, \\ L_A &= \bar{l} \gamma^\mu \gamma_5 l, \\ H_{1\mu} &= \bar{\Lambda} \gamma_\mu (A_1 P_R + B_1 P_L) \Lambda_b + \bar{\Lambda} i \sigma_{\mu\nu} q^\nu (A_2 P_R + B_2 P_L) \Lambda_b, \\ H_{2\mu} &= E_1 \bar{\Lambda} \gamma_\mu P_L \Lambda_b + E_2 \bar{\Lambda} i \sigma_{\mu\nu} q^\nu P_L \Lambda_b + E_3 q_\mu \bar{\Lambda} (P_L \Lambda_b) \end{aligned} \quad (5)$$

where one has

$$\begin{aligned} q &= p_{\Lambda_b} - p_\Lambda = p_+ + p_-, \\ A_i &= -\frac{2m_b}{q^2} C_7 f_i^T, \quad B_i = C_9^{eff} f_i, \quad E_i = C_{10} f_i, \\ f_1 &= f_2^T = F_1 + \sqrt{r} R F_1, \quad f_2 = f_3 = \frac{R F_1}{M_{\Lambda_b}}. \end{aligned} \quad (6)$$

3 Lepton Asymmetries

In this section we present the formulas for the forward-backward and the longitudinal, normal and transverse lepton polarization asymmetries in $\Lambda_b(p_{\Lambda_b}) \rightarrow \Lambda(p_\Lambda)l^+(p_+, s_+)l^-(p_-)$. We shall concentrate on the l^+ spin for the polarizations. To do this, we write the l^+ four-spin vector in terms of a unit vector, $\hat{\xi}$, along the l^+ spin in its rest frame, as

$$s_+^0 = \frac{\vec{p}_+ \cdot \hat{\xi}}{m_l}, \quad \vec{s}_+ = \hat{\xi} + \frac{s_+^0}{E_{l^+} + m_l} \vec{p}_+, \quad (7)$$

and choose the unit vectors along the longitudinal, normal, and transverse components of the l^+ polarization to be

$$\begin{aligned} \hat{e}_L &= \frac{\vec{p}_+}{|\vec{p}_+|}, \\ \hat{e}_N &= \frac{\vec{p}_+ \times (\vec{p}_\Lambda \times \vec{p}_+)}{|\vec{p}_+ \times (\vec{p}_\Lambda \times \vec{p}_+)|}, \\ \hat{e}_T &= \frac{\vec{p}_\Lambda \times \vec{p}_+}{|\vec{p}_\Lambda \times \vec{p}_+|}, \end{aligned} \quad (8)$$

respectively. The partial decay width for $\Lambda_b \rightarrow \Lambda l^+ l^-$ is given by

$$\begin{aligned} d\Gamma &= \frac{1}{4M_{\Lambda_b}} |\mathcal{M}|^2 (2\pi)^4 \delta(p_{\Lambda_b} - p_\Lambda - p_{l^+} - p_{l^-}) \\ &\times \frac{d\vec{p}_\Lambda}{(2\pi)^3 2E_\Lambda} \frac{d\vec{p}_{l^+}}{(2\pi)^3 2E_1} \frac{d\vec{p}_{l^-}}{(2\pi)^3 2E_2} \end{aligned} \quad (9)$$

with

$$|\mathcal{M}|^2 = \frac{1}{2} |\mathcal{M}^0|^2 \left[1 + (P_L \hat{e}_L + P_N \hat{e}_N + P_T \hat{e}_T) \cdot \hat{\xi} \right], \quad (10)$$

where $|\mathcal{M}^0|^2$ is related to the decay rate for the unpolarized l^+ and P_i ($i = L, N, T$) are the longitudinal, normal and transverse polarizations of l^+ , respectively. Introducing dimensionless variables of $\lambda_t = V_{tb}V_{ts}^*$, $r = M_\Lambda^2/M_{\Lambda_b}^2$, $\hat{m}_l = m_l/M_{\Lambda_b}$, $\hat{m}_b = m_b/M_{\Lambda_b}$, $\hat{s} = q^2/M_{\Lambda_b}^2$ and $\hat{t} = p_{\Lambda_b} \cdot p_\Lambda/M_{\Lambda_b}^2 = (1 + r - \hat{s})/2$, using the transition matrix element of Eq. (4), and integrating the angle dependence of the lepton, the differential decay width in Eq. (9) becomes

$$d\Gamma = \frac{1}{2} d\Gamma^0 \left[1 + \vec{P} \cdot \vec{\xi} \right] \quad (11)$$

with

$$d\Gamma^0 = \frac{G_F^2 \alpha_{em}^2 \lambda_t^2}{384\pi^5} M_{\Lambda_b}^5 \sqrt{\phi(\hat{s})} \sqrt{1 - \frac{4\hat{m}_l^2}{\hat{s}}} R_{\Lambda_b}(\hat{s}) d\hat{s} \quad (12)$$

and

$$\vec{P} = P_L \hat{e}_L + P_N \hat{e}_N + P_T \hat{e}_T, \quad (13)$$

where

$$\phi(\hat{s}) = (1 - r)^2 - 2\hat{s}(1 + r) + \hat{s}^2 \quad (14)$$

and

$$\begin{aligned}
R_{\Lambda_b}(\hat{s}) = & 4 \frac{\hat{m}_b^2}{\hat{s}} |C_7|^2 F_1^2 \left\{ - \left(1 - R^2\right) \left[\hat{s} \hat{t} - 4(1 - \hat{t})(\hat{t} - r) \right] \right. \\
& - 2R(\sqrt{r} + R\hat{t}) \left(\hat{s} - 4(1 - \hat{t})^2 \right) + 8 \frac{\hat{m}_l^2}{\hat{s}} \left[\left(1 - R^2\right) (1 - \hat{t})(\hat{t} - r) \right. \\
& \left. + 2R(\sqrt{r} + R\hat{t})(1 - \hat{t})^2 \right] - 2\hat{m}_l^2 \left((1 + R^2) \hat{t} + 2R\sqrt{r} \right) \left. \right\} \\
& + 12\hat{m}_b \text{Re}C_9^{eff} C_7^* \left(1 + 2 \frac{\hat{m}_l^2}{\hat{s}} \right) F_1^2 \left[\left(1 - R^2\right) (\hat{t} - r) + 2R(\sqrt{r} + R\hat{t})(1 - \hat{t}) \right] \\
& + \left(|C_9^{eff}|^2 + |C_{10}|^2 \right) F_1^2 \left\{ \left(1 - 4 \frac{\hat{m}_l^2}{\hat{s}}\right) \left[(1 + R^2) \hat{t} + 2R\sqrt{r} \right] \right. \\
& \left. + 2 \left(1 + 2 \frac{\hat{m}_l^2}{\hat{s}} \right) (1 - \hat{t}) \left[(\hat{t} - r)(1 - R^2) + 2R(\sqrt{r} + R\hat{t})(1 - \hat{t}) \right] \right\}, \\
& + 6\hat{m}_l^2 \left(|C_9^{eff}|^2 - |C_{10}|^2 \right) F_1^2 \left[(1 + R^2) \hat{t} + 2R\sqrt{r} \right]. \tag{15}
\end{aligned}$$

In Eqs. (12) and (15), the allowed range of \hat{s} is

$$4\hat{m}_l^2 \leq \hat{s} \leq (1 - \sqrt{r})^2. \tag{16}$$

Defining the longitudinal, normal and transverse l^+ polarization asymmetries by

$$P_i(\hat{s}) = \frac{d\Gamma(\hat{e}_i \cdot \hat{\xi} = 1) - d\Gamma(\hat{e}_i \cdot \hat{\xi} = -1)}{d\Gamma(\hat{e}_i \cdot \hat{\xi} = 1) + d\Gamma(\hat{e}_i \cdot \hat{\xi} = -1)}, \tag{17}$$

from Eq. (11) we find that

$$P_L(\hat{s}) = -\sqrt{1 - \frac{4\hat{m}_l^2}{\hat{s}}} \frac{R_L(\hat{s})}{R_{\Lambda_b}(\hat{s})}, \tag{18}$$

$$P_N(\hat{s}) = \frac{3}{4} \pi \hat{m}_l \sqrt{\frac{\phi(\hat{s})}{\hat{s}}} \frac{R_N(\hat{s})}{R_{\Lambda_b}(\hat{s})}, \tag{19}$$

$$P_T(\hat{s}) = \frac{3}{4} \pi \hat{m}_l \sqrt{\hat{s} \phi(\hat{s})} \sqrt{1 - \frac{4\hat{m}_l^2}{\hat{s}}} \frac{R_T(\hat{s})}{R_{\Lambda_b}(\hat{s})}, \tag{20}$$

where

$$\begin{aligned}
R_L(\hat{s}) = & F_1^2 \text{Re}C_9^{eff} C_{10}^* \left[\left(1 - R^2\right) \left((1 - r)^2 + \hat{s}(1 + r) - 2\hat{s}^2 \right) \right. \\
& \left. + 2R(\sqrt{r} + R\hat{t}) \left(2\hat{s} + (1 - r + \hat{s})^2 \right) \right] \\
& + 6F_1^2 \text{Re}C_{10} C_7^* \hat{m}_b \left[(1 - r - \hat{s})(1 - R^2) + 2R(\sqrt{r} + R\hat{t})(1 - r + \hat{s}) \right], \\
R_N(\hat{s}) = & 4F_1^2 \frac{\hat{m}_b^2}{\hat{s}} |C_7|^2 \left[\left(1 - R^2\right) (1 - r) + 2R(\sqrt{r} + R\hat{t})(1 - r + s) \right] \\
& + F_1^2 \left(1 - R^2\right) |C_9^{eff}|^2 \hat{s} + F_1^2 \text{Re}C_9^{eff} C_{10}^* \left[(1 - r)(1 - R^2) \right. \\
& \left. + 2(1 - r + \hat{s})R(\sqrt{r} + R\hat{t}) \right] \\
& + 2F_1^2 \hat{m}_b \left(2\text{Re}C_9^{eff} C_7^* + \text{Re}C_{10} C_7^* \right) \left(1 - R^2 + 2R(\sqrt{r} + R\hat{t}) \right), \\
R_T(\hat{s}) = & F_1^2 \frac{2\hat{m}_b}{\hat{s}} \text{Im}C_7 C_{10}^* \left(1 - R^2 + 2R(\sqrt{r} + R\hat{t}) \right) + F_1^2 \text{Im}C_9^{eff} C_{10}^* \left(1 - R^2 \right). \tag{21}
\end{aligned}$$

We note that the transverse part of the lepton polarization in Eq. (20) is a T-odd observable.

The differential and normalized dilepton forward-backward asymmetries (FBAs) for the decay of $\Lambda_b \rightarrow \Lambda l^+ l^-$ as a function of \hat{s} are defined by

$$\frac{dA_{FB}(\hat{s})}{d\hat{s}} = \left[\int_0^1 d\cos\theta \frac{d^2\Gamma(\hat{s})}{d\hat{s}d\cos\theta} - \int_{-1}^0 d\cos\theta \frac{d^2\Gamma(\hat{s})}{d\hat{s}d\cos\theta} \right] \quad (22)$$

and

$$\mathcal{A}_{FB}(\hat{s}) = \frac{1}{d\Gamma(\hat{s})/d\hat{s}} \left[\int_0^1 d\cos\theta \frac{d^2\Gamma(\hat{s})}{d\hat{s}d\cos\theta} - \int_{-1}^0 d\cos\theta \frac{d^2\Gamma(\hat{s})}{d\hat{s}d\cos\theta} \right], \quad (23)$$

respectively, where θ is the angle of l^+ with respect to Λ_b in the rest frame of the lepton pair. Explicitly, we obtain

$$\frac{dA_{FB}(\hat{s})}{d\hat{s}} = \frac{G_F^2 \alpha_{em}^2 \lambda_t^2}{2^8 \pi^5} M_{\Lambda_b}^5 \phi(\hat{s}) \left(1 - 4 \frac{\hat{m}_l^2}{\hat{s}} \right) R_{FB}(\hat{s}) \quad (24)$$

and

$$\mathcal{A}_{FB}(\hat{s}) = \frac{3}{2} \sqrt{\phi(\hat{s})} \sqrt{1 - \frac{4\hat{m}_l^2}{s}} \frac{R_{FB}(\hat{s})}{R_{\Lambda_b}(\hat{s})} \quad (25)$$

where

$$R_{FB}(\hat{s}) = F_1^2(1 - R^2) \left[2\hat{m}_b \text{Re}C_{10}C_7^* \left(1 + 2 \frac{R\sqrt{r} + R^2\hat{t}}{1 - R^2} \right) + \hat{s} \text{Re}C_9^{eff}C_{10}^* \right]. \quad (26)$$

From Eqs. (15), (18)-(21), and (25)-(26), we see that P_i ($i = L, N, T$) and \mathcal{A}_{FB} depend only on R since the factor F_1^2 is canceled out. Thus, once one gets the value of R , the only uncertainty for the asymmetries is from the Wilson coefficients. It is interesting to note that these asymmetries are sensitive to the chiral structure of electroweak interactions since they are related to the products of $C_9C_7^*$, $C_{10}C_7^*$ and $C_9C_{10}^*$.

4 Numerical Analysis

In our numerical calculations, the Wilson coefficients are evaluated at the scale $\mu \simeq m_b$ and the other parameters are listed in Table 1 of Ref. [8]. For the form factors in the $\Lambda_b \rightarrow \Lambda$ transition, we use the results from both the QCD sum rule approach [6] and the pole model [9]. In the QCD sum rule approach we use the form

$$F_i(q^2) = \frac{F_i(0)}{1 + aq^2 + bq^4}, \quad (27)$$

where the parameters in Eq. (27) are shown in Table 1. From the Table, we find that $R(0) = F_2(0)/F_1(0) = -0.17$ and $R(q_{\max}^2) = -0.44$ which are consistent with the CLEO result of $R = -0.25 \pm 0.14 \pm 0.08$ [14]. In the pole model, we adopt

$$F_i(q^2) = N_i \left(\frac{\Lambda_{QCD}}{\Lambda_{QCD} + z} \right)^2 \quad (28)$$

where $z = p_\Lambda \cdot p_{\Lambda_b} / M_{\Lambda_b} = (1 + r - q^2/M_{\Lambda_b}^2) M_{\Lambda_b} / 2$ and Λ_{QCD} is chosen around 200 MeV. Assuming the form factors for the transition of $\Lambda_c \rightarrow \Lambda$ are similar to that of $\Lambda_b \rightarrow \Lambda$ and using $R = -0.25$ [14] and the branching ratio of $\Lambda_c^+ \rightarrow \Lambda e^+ \nu_e$, we obtain that $N_{1,2}$ are $(52.32, -13.08)$ [8].

Table 1: Form Factors in the QCD sum rule approach.

	F_1	F_2
$q^2 = 0$	0.462	-0.077
a	-0.0182	-0.0685
b	-0.000176	0.00146

4.1 Forward-backward Asymmetries

From Eqs. (24) and (25), we see that the FBAs for the light charged lepton modes of $\Lambda_b \rightarrow \Lambda l^+ l^-$ ($l = e$ and μ) are close to each other. As a result, we shall not mention the electron mode of $\Lambda_b \rightarrow \Lambda e^+ e^-$. In Figures 1 and 2, we show $\mathcal{A}_{FB}(\Lambda_b \rightarrow \Lambda l^+ l^-)$ as a function of dimensionless variable \hat{s} for $l = \mu$ and τ , respectively. From Figure 1(a), we see that $\mathcal{A}_{FB}(\Lambda_b \rightarrow \Lambda \mu^+ \mu^-)$ has a zero value at \hat{s}_0 which satisfies the condition

$$ReC_9^{eff}C_{10}^* = -\frac{2\hat{m}_b}{\hat{s}_0} ReC_7C_{10}^* \frac{1 - R^2 + 2R(\sqrt{r} + R\hat{t})}{(1 - R^2)}. \quad (29)$$

Furthermore, we find that the contributions from the pole and QCD sum rule models to FBAs overlap at the low q^2 region so that in both models Eq. (29) can be simplified to

$$ReC_9^{eff}C_{10}^* \simeq -\frac{2\hat{m}_b}{\hat{s}_0} ReC_7C_{10}^*, \quad (30)$$

which is independent of the hadronic form factors. Explicitly, from Figure 1(a), in the standard model we get that \hat{s}_0 is 0.109 and 0.114 with and without R terms for excluding LD effects, and 0.098 and 0.102 for including LD effects, respectively. It is clear that the zero point of $\mathcal{A}_{FB}(\Lambda_b \rightarrow \Lambda \mu^+ \mu^-)$ is mainly affected by the weak Wilson coefficients of C_7 and C_9 that are sensitive to physics beyond the standard model. For example, if one of C_7 and C_9 has an opposite sign to that in the standard model, the condition for the zero point in Eq. (30) will not be satisfied. Therefore, measuring a sizable value of the FBA around \hat{s}_0 is a clear indication of new physics. This result is similar to $B \rightarrow K^* l^+ l^-$ decays mentioned by [15] with large energy effective theory (LEET) [16]. We note that the vanishing of the FBAs in the inclusive decays of $b \rightarrow (s, d) l^+ l^-$ and the exclusive ones of $B \rightarrow (K^*, \rho) l^+ l^-$ were first studied by Burdman [17]. Our conclusion for the baryonic decays coincides with that in Ref. [17].

From the figures, we find that there is no much difference for the FBAs between the QCD sum rule approach and the pole model at the lower values of q^2 , especially for that in the muon mode. By taking R to be zero, the distributions for both models in Figures 1 and 2 should be identical. Thus, the differences for the FBAs in the different QCD models actually reflect the effects of the ratio R . The insensitivity to the form factors for the FBAs provides us a candidate to test the standard model.

In Figure 3, we show the differential FBA of $d\mathcal{A}_{FB}(\hat{s})/d\hat{s}$ which, unlike \mathcal{A}_{FB} , is insensitive to R . This can be understood that due to Eqs. (24) and (25) it is proportional to $R_{FB}(\hat{s})$ in which the terms with F_1^2 are the dominant contributions and those with R are negligible since these terms are related to either R^2 or $R\sqrt{r}$, which are small.

We now define the integrated FBA to be

$$\bar{\mathcal{A}}_{FB} = \int_{4\hat{m}_l^2}^{\hat{s}_{\max}} d\hat{s} \mathcal{A}_{FB}(\hat{s}) \quad (31)$$

where $\hat{s}_{\max} = (1 - \sqrt{r})^2$. Without LD contributions, in the standard model we find that

$$\bar{\mathcal{A}}_{FB}(\Lambda_b \rightarrow \Lambda \mu^+ \mu^-) = -0.13 \text{ } (-0.12) \quad (32)$$

and

$$\bar{\mathcal{A}}_{FB}(\Lambda_b \rightarrow \Lambda \tau^+ \tau^-) = -0.04 \text{ } (-0.03) \quad (33)$$

for the QCD sum rule approach (pole model), respectively.

4.2 Polarization Asymmetries

We now discuss the longitudinal, normal and transverse polarization asymmetries of the lepton and their implications. From Eqs. (18)–(20), the distributions of P_L , P_N and P_T with respect to the dimensionless kinematic variable \hat{s} are shown in Figures 4–9, respectively. From the figures, we find that the results of the QCD sum rule and pole models to various polarizations are as follows: (1) they overlap fully for P_L ; (2) P_N is not sensitive to the models except for the small q^2 region in $\Lambda_b \rightarrow \Lambda \mu^+ \mu^-$; and (3) the effects of the different QCD models to P_T are significant at the large q^2 region. Clearly, P_L and P_N for the most q^2 region in $\Lambda_b \rightarrow \Lambda l^+ l^-$ are independent of the QCD models.

It is easily seen that outside the resonant states, both polarizations of P_L and P_N are insensitive to the LD effects. We note that P_L for $\Lambda_b \rightarrow \Lambda \mu^+ \mu^-$ is close to 1, while that for the tau mode is over 40%, in the most values of q^2 except that around resonant regions. The large asymmetries in $\Lambda_b \rightarrow \Lambda l^+ l^-$ are good candidates to test the standard model. For P_T , since it is proportional to the imaginary parts of the Wilson coefficient products, the LD contributions are important. Note that in the standard model, the effective Wilson coefficients of C_9^{eff} contains absorptive parts, while C_7 and C_{10} have only real values. From Eq. (20), the part of $Im(C_9^{eff} C_{10}^*)$ yields a nonzero value of P_T , but that of $Im(C_7 C_{10}^*)$ vanishes. However, due to the enhanced factor $1/\hat{s}$ at small \hat{s} for the term corresponding to $Im(C_7 C_{10}^*)$, one could search for these regions since the contribution from some non-standard CP violation model may not be negligible.

Finally, in Table 2, we list the integrated lepton polarization asymmetries in $\Lambda_b \rightarrow \Lambda l^+ l^-$, defined by

$$\bar{P}_i = \int_{4\hat{m}_l^2}^{\hat{s}_{\max}} d\hat{s} P_i. \quad (34)$$

In the table, the results are calculated in the standard model without LD effects.

5 Conclusions

We have given a detailed analysis on the dilepton forward-backward and the longitudinal, normal and transverse lepton polarization asymmetries for the decays of $\Lambda_b \rightarrow \Lambda l^+ l^-$ ($l =$

Table 2: Integrated lepton polarization asymmetries in the standard model without LD effects.

Model	Mode	$10^2 \bar{P}_L$	$10^2 \bar{P}_N$	$10^2 \bar{P}_T$
QCD sum rule	$\Lambda_b \rightarrow \Lambda \mu^+ \mu^-$	58.3	-9.4	-0.07
	$\Lambda_b \rightarrow \Lambda \tau^+ \tau^-$	10.9	-10.0	-0.39
pole model	$\Lambda_b \rightarrow \Lambda \mu^+ \mu^-$	58.3	-12.6	-0.07
	$\Lambda_b \rightarrow \Lambda \tau^+ \tau^-$	10.9	-9.2	-0.34

e, μ, τ) in the standard model. Based on the HQET, there are only two independent form factors, F_1 and F_2 or F_1 and R , involved in the matrix element of $\Lambda_b \rightarrow \Lambda$.

We have shown that all the asymmetries are related to R and free of the other form factor F_1 . Moreover, we have found that R is always associated with \sqrt{r} so that by neglecting their contributions, there are only a few percentages lose in the asymmetries. Thus, the asymmetries in the heavy baryonic dilepton decays have a less dependence on the non-perturbative QCD effects. We have also demonstrated that $P_L(\Lambda_b \rightarrow \Lambda l^+ l^-)$ are QCD model independent quantities. We have pointed out that the FBA for the light lepton mode gets to zero at \hat{s}_0 which is only sensitive to the weak couplings. Finally, since the absolute values of the integrated T-odd observables of the transverse lepton polarizations in $\Lambda_b \rightarrow \Lambda l^+ l^-$ are less than 10^{-2} in the standard model, measuring P_T such as in the tau model at a level of 10^{-2} would be a clear signal for some new CP violation.

Acknowledgments

This work was supported in part by the National Science Council of the Republic of China under contract numbers NSC-89-2112-M-007-054 and NSC-89-2112-M-006-033.

References

- [1] A. Ali, T. Mannel, and T. Morozumi, *Phys. Lett.* **B273**, 505 (1991).
- [2] J. L. Hewett, *Phys. Rev.* **D53**, 4964 (1996).
- [3] F. Krüger and L.M. Sehgal, *Phys. Lett.* **B380**, 199 (1996).
- [4] C.Q. Geng and C. P. Kao, *Phys. Rev.* **D54**, 5636 (1996).
- [5] C.Q. Geng and C. P. Kao, *Phys. Rev.* **D57**, 4479 (1998).
- [6] Chao-Shang Huang and Hua-Gang Yan, *Phys Rev.* **D59**, 114022 (1999).
- [7] Chuan-Hung Chen and C. Q. Geng, hep-ph/0012003, to be published in *Phys Rev.* **D**.
- [8] Chuan-Hung Chen and C. Q. Geng, hep-ph/0101171.
- [9] T. Mannel, W. Roberts and Z. Ryzak *Nucl. Phys.* **B355**, 38 (1991); T. Mannel and S. Recksiegel *J. Phys.* **G24**, 979 (1998).
- [10] G. Buchalla, A. J. Buras and M. E. Lautenbacher, *Rev. Mod. Phys.* **68**, 1230 (1996).
- [11] N.G. Deshpande, J. Trampetic and K. Panose, *Phys. Rev.* **D39**, 1462 (1989).
- [12] C.S. Lim, T. Morozumi, and A.T. Sanda, *Phys. Lett.* **B218**, 343 (1989).
- [13] P.J. O'Donnell and K.K.K. Tung, *Phys. Rev.* **D43**, R2067 (1991).
- [14] CLEO Collaboration, G. Crawford *et al* *Phys. Rev. Lett.* **75**, 624 (1995).
- [15] A. Ali, P. Ball, L.T. Handoko, and G. Hiller, *Phys. Rev.* **D61**, 074024 (2000).
- [16] J. Charles, A.L. Yaouanc, L. Oliver, O. Pène, and J.C. Raynal, *Phys. Rev.* **D60**, 014001 (1999).
- [17] G. Burdman, *Phys. Rev.* **D57**, 4254 (1998).

Figure Captions

Figure 1: FBAs as a function of $q^2/M_{\Lambda_b}^2$ for (a) $\Lambda_b \rightarrow \Lambda\mu^+\mu^-$ and (b) $\Lambda_b \rightarrow \Lambda\tau^+\tau^-$. The curves with and without resonant shapes represent including and no LD contributions, respectively. The solid (dash-dotted) curves stand for the QCD sum rule approach and the dashed (dotted) for the pole model with (without) R , respectively.

Figure 2: The differential FBA of dA_{FB}/dq^2 for $\Lambda_b \rightarrow \Lambda\mu^+\mu^-$ as a function of q^2 . Legend is the same as Figure 1.

Figure 3: Longitudinal polarization asymmetries. Legend is the same as Figure 1.

Figure 4: Normal polarization asymmetries. Legend is the same as Figure 1.

Figure 5: Transverse polarization asymmetries. Legend is the same as Figure 1.

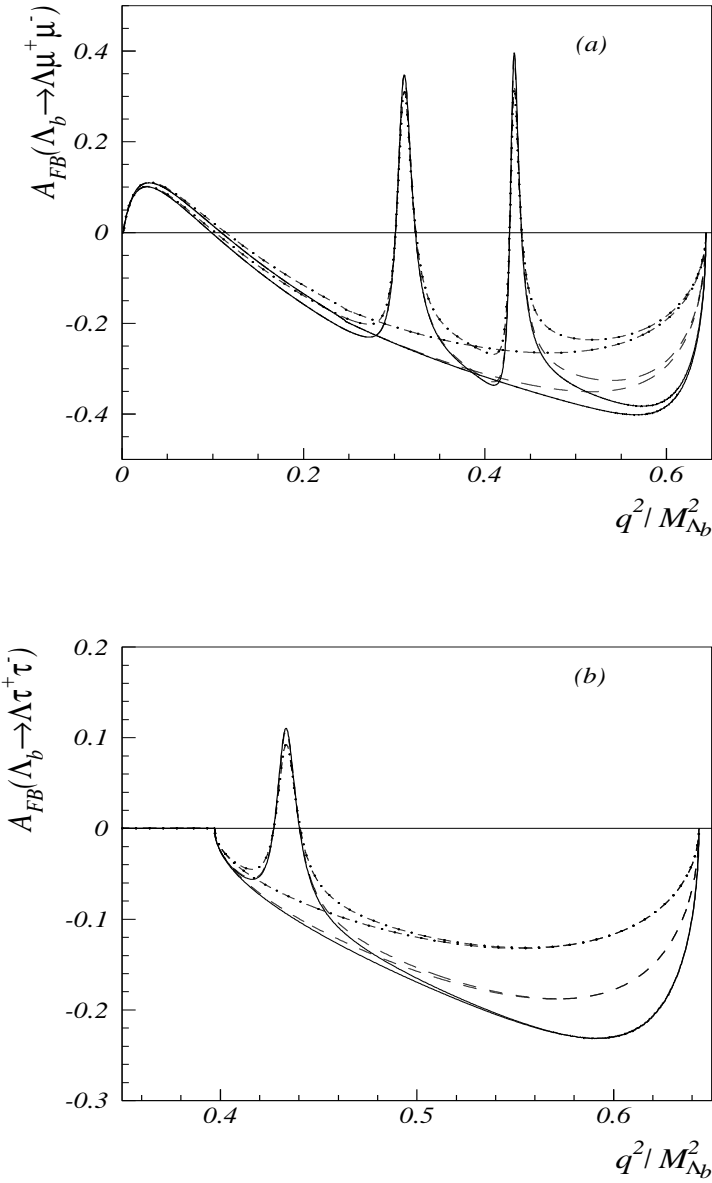


Figure 1: FBAs as a function of $q^2/M_{\Lambda_b}^2$ for (a) $\Lambda_b \rightarrow \Lambda \mu^+ \mu^-$ and (b) $\Lambda_b \rightarrow \Lambda \tau^+ \tau^-$. The curves with and without resonant shapes represent including and no LD contributions, respectively. The solid (dash-dotted) curves stand for the QCD sum rule approach and the dashed (dotted) for the pole model with (without) R , respectively.

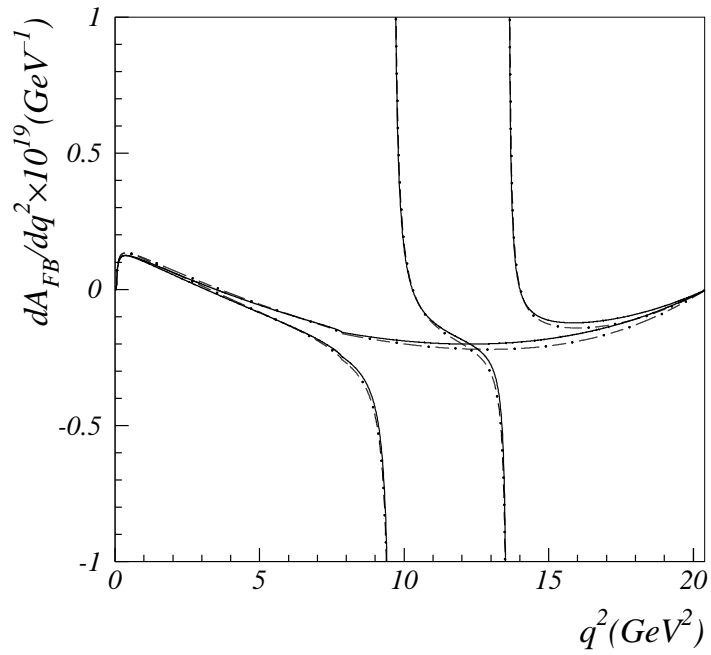


Figure 2: The differential FBA of dA_{FB}/dq^2 for $\Lambda_b \rightarrow \Lambda \mu^+ \mu^-$ as a function of q^2 . Legend is the same as Figure 1.

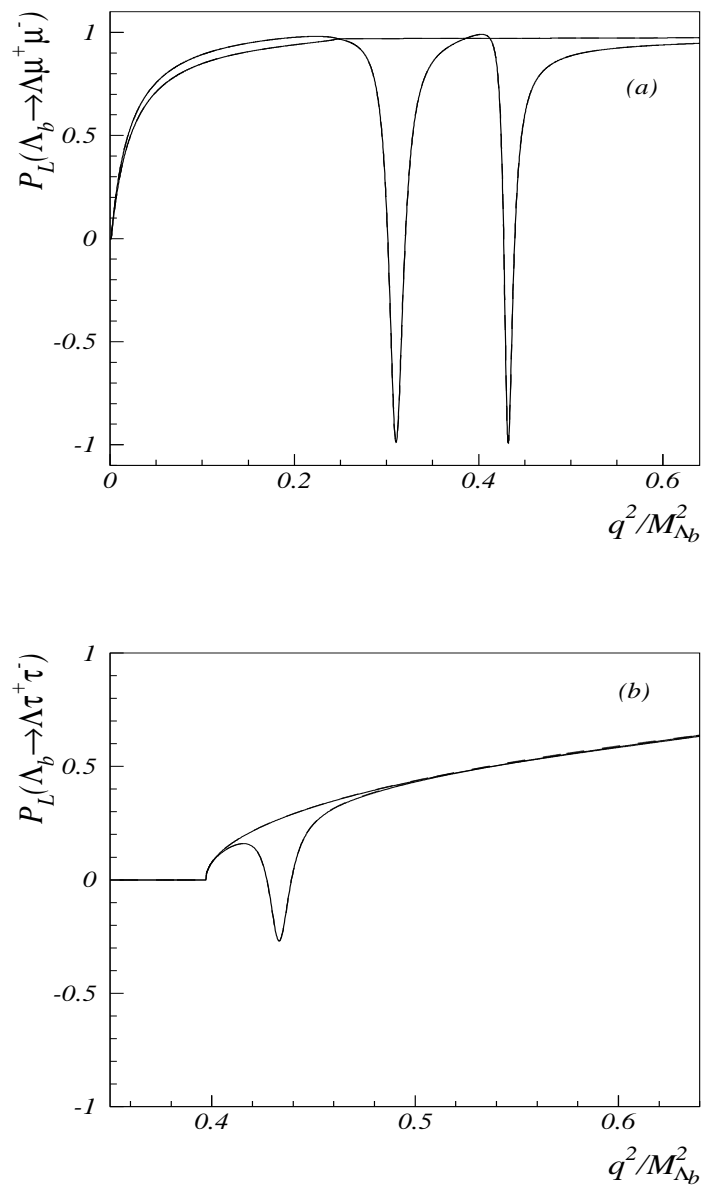


Figure 3: Longitudinal polarization asymmetries. Legend is the same as Figure 1.

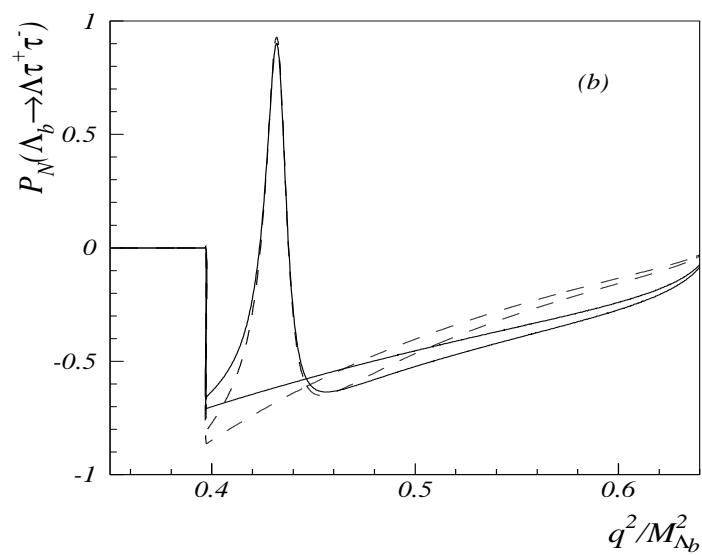
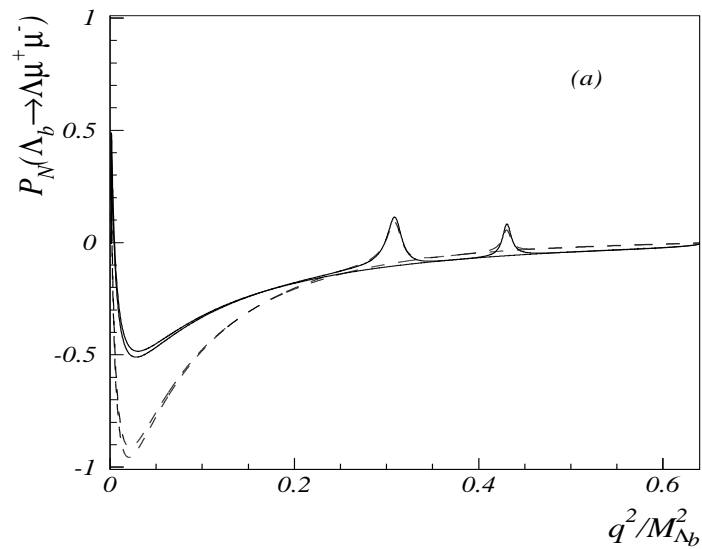


Figure 4: Normal polarization asymmetries. Legend is the same as Figure 1.

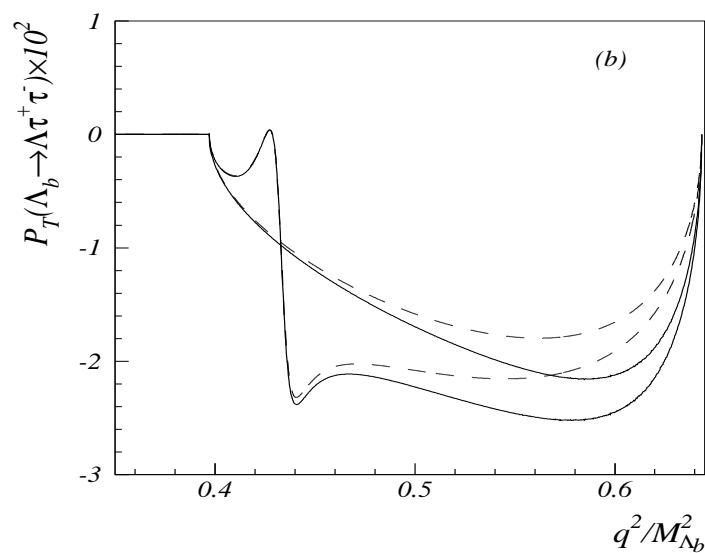
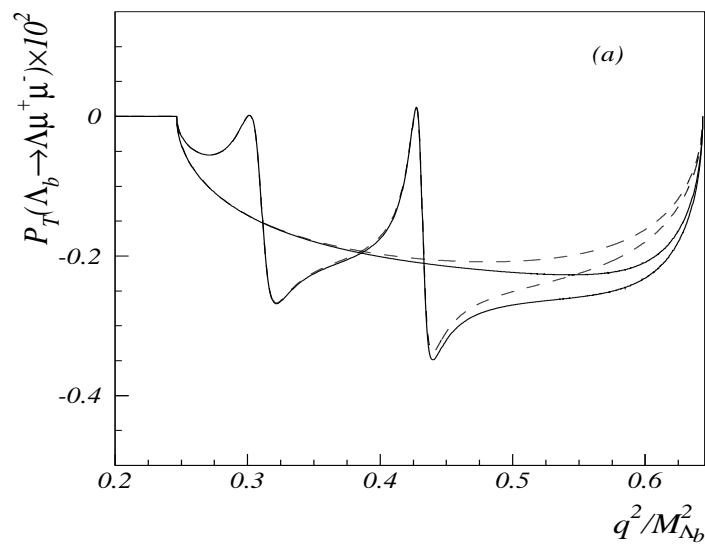


Figure 5: Transverse polarization asymmetries. Legend is the same as Figure 1.